

“INFRARED SPECTROSCOPIC VIEW OF POLLUTANT AEROSOL”

By 1.RAJ KISHOR YADAV

PhD Scholar (Chemistry). HGU UTTARAKHAND

2. Dr DUSHYANT Associate professor

Department of Chemistry H.G.U

ABSTRACT

Hygroscopic nature is to circulate water molecule formulating bond with their molecule by the adsorbent such as sodium nitrate, silica gel, alumina etc .Aerosol is heterogeneous mixture of air and solid particulate but, their qualitative analysis is done by IR spectroscopy . The Fourier-transform infrared (FT-IR) spectra of ambient fine aerosols were formulated with partial least-squares (PLS)¹. This review is based on air pollution level, meteorological conditions, and aerosol optical and radiation characteristics relative humidity in different circulation patterns .

INTRODUCTION

Infrared spectroscopy was used to classify dry aerosol particles . Direct measurements of the aerosol particle size agree with size spectra retrieved from inversion of the extinction measurements using Mie calculations, where the difference residual value is in the order of 0.2%.deduction .Fourier-transform infrared (FTIR) ² spectroscopy is a powerful spectral detection technology . FTIR spectra are composed of absorption peaks generated from infrared radiation absorption during the vibration transition of asymmetric dipole moment ³polyatomic molecules, and a wide variety of gaseous pollutants can be measured by FTIR technology due to their physical structures. FTIR has high sensitivity, permitting the detection of changes in gas concentration at the ppb (parts per billion, volume concentration) level. Open-path FTIR have been applied to the online detection of trace gas emissions from forest fires ⁴ and soil during the burning of crop, from traffic emissions along highways road and in harbors . The identification of each component in the FTIR spectrum is crucial for accurate quantitative analysis and control. In the early stage of FTIR spectrum identification, library searching (LS) methods were adopted when the spectral components were single or the absorption peaks rarely overlapped. Due to the strong abilities of curve fitting and anti-interference of the artificial neural network (ANN), a variety of ANN-based FTIR spectrum⁵ identification algorithms is done. However, due to the complexity of atmospheric gaseous compositions and water vapor interference in the actual measured spectra, there are few studies where ICA⁶ is applied to the component identification of atmospheric gaseous pollutant spectra. Humidity affects the natural deposition of particulate matter in the atmosphere. With an increase in humidity, particulate size also increases due to hygroscopic nature and it becomes too heavy to remain in the air and begins to fall off. This is called the dry deposition of particulate⁷ matter..

In this study, we conducted identification experiments on the spectra collected both in the laboratory and in the actual atmosphere. The infrared spectra⁸ were collected by extraction FTIR gas spectrometer independently developed by CAS, with a multi pass gas cell of a 10 m optical path inside. The spectrometer has a measuring band width of 500 cm⁻¹–5000 cm⁻¹ and spectral resolution of 1 cm⁻¹ wave number. Methane (CH₄), ethanol (C₂H₅OH), ethyne (C₂H₂), and ethylene (C₂H₄) are common air pollutants. Because of their low cost, simple preparation, and seriously overlapping their infrared absorption bands all these four gases are as the experimental gases .The gas distribution platform can simultaneously distribute four gases⁹ and get the required concentration by adjusting the volume ratio of the auxiliary gas such as nitrogen and the pure gas. In total, we

got 12 samples of mixed gases, the concentration changes of four gases in different samples are mutually independence and this is a necessary condition for ICA separation. In order to simulate the composition of pollutants in the atmosphere, the concentrations of the gases were controlled below 60 ppm concentration.

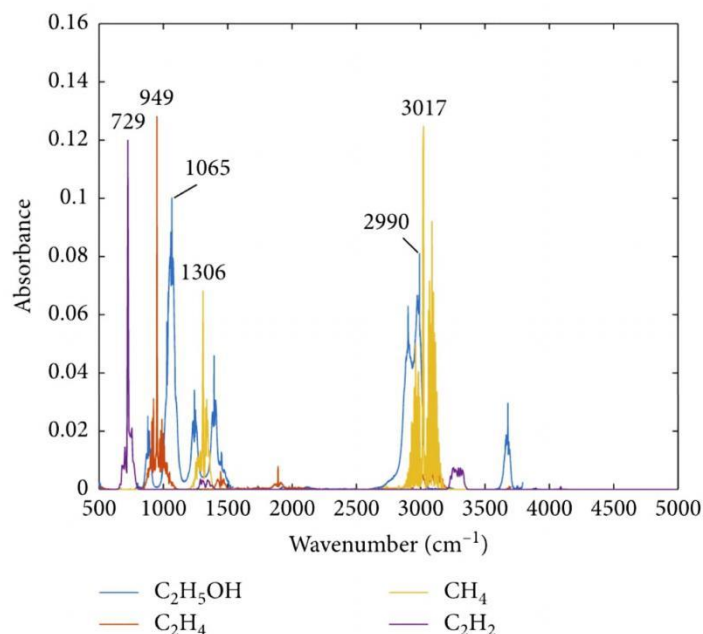


Fig 1. Absorbance spectrum

Before spectra acquisition, the gas storage cylinders were placed in a ventilation room to avoid dangerous gas leakage, all the experimental system and the connecting pipes were completely sealed, and a tightness test was performed. The four gases and nitrogen were configured to the concentrations as required by the software built into the gas distribution platform. The spectra were recorded at stable barometric pressure. Absorption¹⁰ bands are specified as below

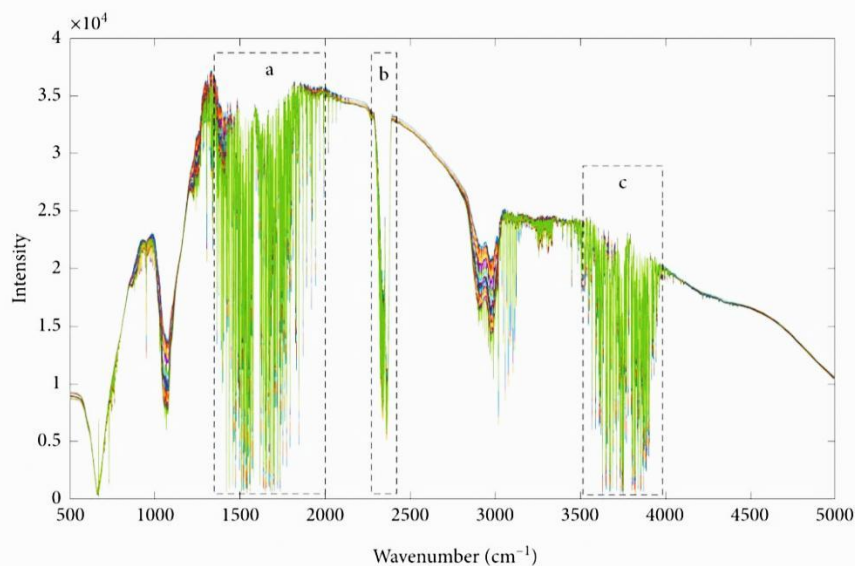


Fig 2 a ,c are absorption band of H₂O and c is absorption band of CO₂

De-noised spectra of 12 groups mixed experimental gases. (a) and (c) are the absorption bands of H₂O. where (b) is the absorption band of CO₂. In addition to the absorption peaks of experimental gases, water vapor and carbon dioxide¹¹ also have strong absorption bands in raw spectra. CO₂ and H₂O (g) produce serious interference in the analysis of atmospheric¹⁰ infrared spectra. As we can see from Figure 3, that H₂O (g) has strong and wide absorption peaks in the range of 1350 cm⁻¹ to 1800 cm⁻¹ and 3500 cm⁻¹ to 3900 cm⁻¹, CO₂ gets

strong absorption peaks in the range of 2280 cm^{-1} to 2385 cm^{-1} . When using FTIR to analyze gaseous components, the common method to avoid the interference of $\text{H}_2\text{O (g)}$ is to analyze the gaseous components in the “infrared atmospheric window” that is far away from the $\text{H}_2\text{O (g)}$ absorption wavebands. Based on this idea, we remove the strong absorption bands of $\text{H}_2\text{O (g)}$ and CO_2 from the spectra and connect the rest of the waveband together. The elimination of interference of water vapor¹² and carbon dioxide before implementing the identification procedure can greatly reduce the complexity of gas analysis.

FTIR Spectra Acquisition of Atmospheric pollutant

There is no large-scale chemical industry source, and the atmospheric gaseous pollutants usually come from the exhaust gas of automobiles and factories contain a variety of toxic and harmful gases, including CO , CO_2 , and VOCs like benzene¹³, alkenes, and aromatic hydrocarbon. Because of these VOCs all contain hydrocarbon bond functional groups, they have absorption peaks in the range of 2800 cm^{-1} – 3200 cm^{-1} , and these absorption peaks are similar in spectral profile; hence, it is difficult for traditional identification methods to effectively distinguish the specific component information in the overlapped spectrum¹⁴. In this study, spectral data in the region from 2800 cm^{-1} to 3200 cm^{-1} were used for components identification.

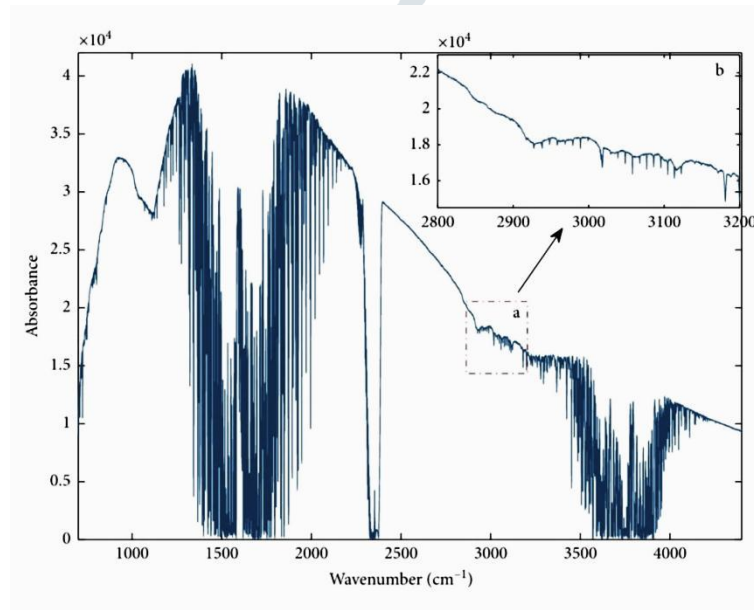


Fig 3. one of the measured atmospheric spectra.

ICA (Independent Components Analysis)

ICA¹⁵ is a powerful signal processing tool, which can restore the original source signal from a set of observed mixed signal; it aims at finding a separation matrix that can transform the observed signal into a linear combination of mutually independent components, which are close to the source signal. The noise-free ICA model can be expressed by the following linear relationship:

$$\mathbf{X} = \mathbf{AS}$$

Where \mathbf{X} denotes the observed m -dimensional signal vector,

\mathbf{S} is an n -dimensional source component vector,

and \mathbf{A} denotes the unknown mixing matrix. ICA attempts to find the optimal separation matrix \mathbf{W} to make the components of \mathbf{S} as independent as possible. Because the source signals and mixing information are unknown, the implementation of ICA requires two important restrictions

- (1) The components of the source signal need to be statistically independent.
- (2) At most one component of the source signal obeys the Gaussian distribution.

The concentration and existence of different gaseous pollutants¹⁶ in the atmosphere rarely appear in proportion to each other, and the spectral signal is not subject to the Gaussian distribution. Therefore, ICA can be used in the separation of spectral signals of atmospheric gaseous pollutants. ICA can efficiently separate original signals from the mixed system, which is linear. We need to make sure that the system is under the assumption of a linear mixture model before we do the analysis. The Beer–Lambert law and absorbance addition describe the relationship between the absorption intensity of multicomponent spectra and the concentration of each light-absorbing substance. The basic principles can be described as follows:

$$A_{total}(\nu) = a_1(\nu)c_1l + a_2(\nu)c_2l + \dots + a_m(\nu)c_ml$$

where $A_{total}(\nu)$ is the total absorption intensity of the spectrum at a certain wavelength ν , $a_i(\nu)$ is the absorption coefficient, c_i is the concentration of component i at wavelength ν , and l is the optical path length. According to the absorbance addition, the absorbance of multicomponent spectrum is the sum of absorbance of each component, and the change of concentration of the component will only cause the change of absorbance amplitude but not the position of absorption peaks and the spectral profile. From the above analysis, we can know that the absorption intensity of atmospheric spectra conforms to the linear model, and the ICA algorithm can be used to separate the spectra of mixed gases.

We obtained the transmittance spectra from FTIR spectrometer. The transmittance information should be converted into absorbance information so that the separation algorithm can analyze the experimental data. The Beer–Lambert law¹⁷ also states the relationship between transmittance $T(\nu)$ and absorbance $A(\nu)$

$$A = \log_{10}(I/T)$$

The identification of separated spectra is achieved through peak searching and comparing the similarity among separated spectra and the standard spectral database. Table 1 lists the infrared absorption characteristics of the four experimental gases from standard spectra database.

Table

Gases	Absorption band (cm ⁻¹)
acetylene	705-760
ethylene	860-1040
ethanol	1050-1240
methane	190-1400

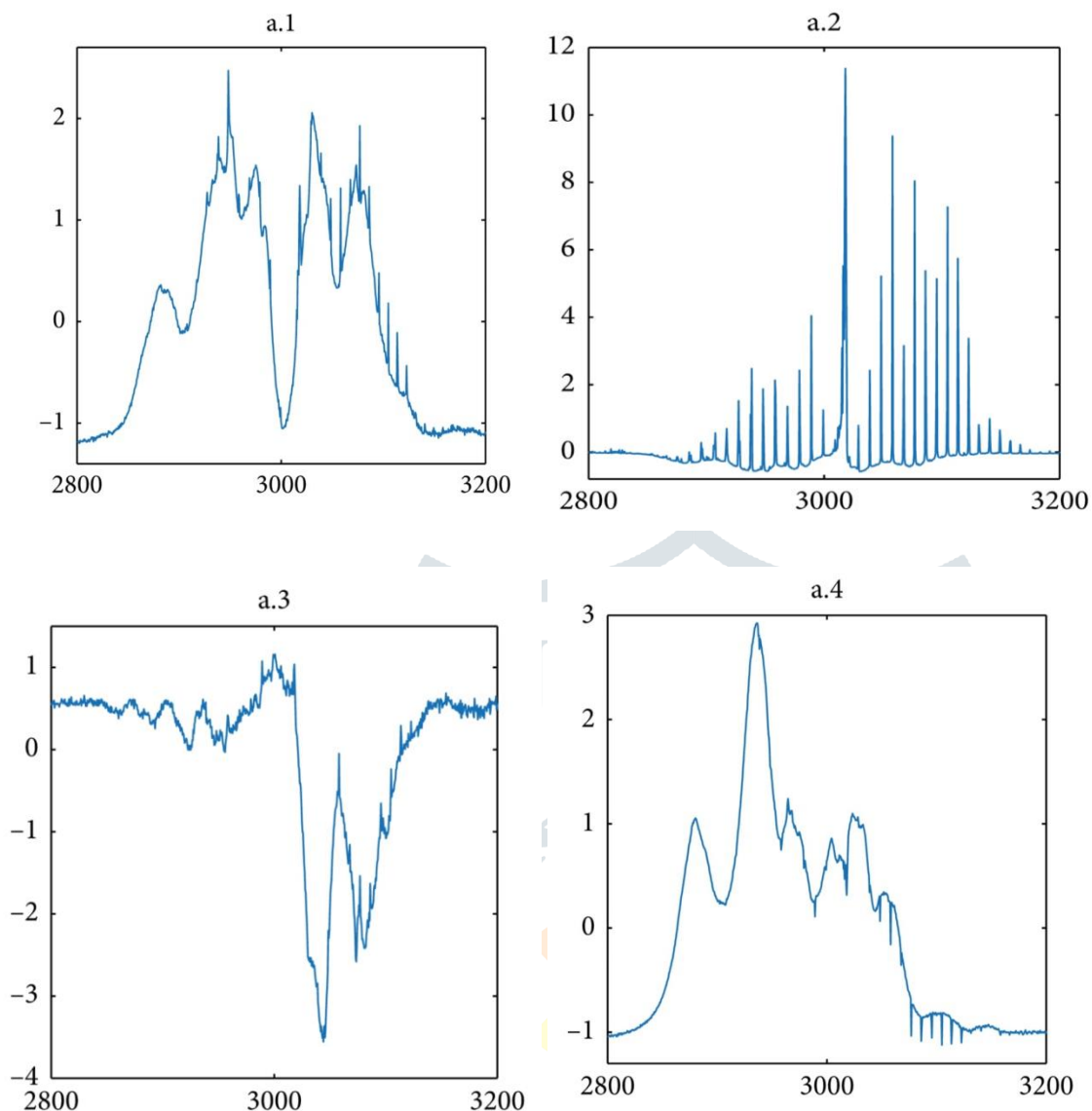


Fig 4. Infrared absorption characteristics of the four gases.

Because the spectrum may produce wavenumber drift¹⁸ in the actual measurement process, it is necessary to set an offset of peak position for peak searching. Generally, the wavenumber drift will not be greater than 1 cm^{-1} , and therefore, we set the peak position offset to 1 cm^{-1} .

This shows the peak searching results of the separated spectra; the peak positions are obtained from the maximum value of absorption bands. By sorting the absorption peaks, the positions of the first two peaks are listed in the table. The gas (or gases) that the spectrum may correspond to is discriminated by the position of the strongest peak, and the sub-strong peak¹⁹ is used to assist this discrimination.

Results

The peak searching results show that most of the possible gases can be recognized by the strongest absorption peak of the separated spectrum, especially the spectrum with a single absorption peak like C_2H_2 and CH_4 . In the first separated spectrum of group (b), there are two absorption peaks with a similar amplitude, corresponding to two possible gases. In this case, the comparison of spectra is necessary for accurate identification.

Based on the results of peak searching, the final identification is completed by analyzing the similarity between the possible components and the corresponding standard spectrum. The correlation coefficient is a measure of

the closeness degree between two column vectors and is used here for spectra similarity discrimination. The correlation²⁰ coefficient r between the standard absorbance spectrum x and the spectrum y to be identified is as follows:

where N is the number of data points in the spectra, and are the mean values of x and y . $-1 \leq r \leq 1$ can be obtained from the definition. According to the previous study [36], the two spectra match well when $r > 0.9$. A further criterion is required for the spectral identification when $r \leq 0.8$. All values of rare greater than 0.8, which means that the separated spectra match well with the standard spectra. The highest correlation is observed with CH_4 , whose r values are all greater than 0.98. Meanwhile, the lowest correlation is observed with $\text{C}_2\text{H}_5\text{OH}$, whose r values are in the range of 0.8259–0.9213. This may be because the absorption bands of CH_4 do not overlap with the absorption bands of H_2O and CO_2 , whereas the absorption bands of $\text{C}_2\text{H}_5\text{OH}$ are complex and part of them overlap²¹ with the absorption band of H_2O , which is removed before the separation. The first spectrum of Figure 8(b) has two corresponding gases according to peak searching, and the spectrum can be identified by calculating the correlation coefficient between this spectrum and the standard spectrum of the two possible gases. The r value is 0.4126 for CH_4 and 0.8259 for $\text{C}_2\text{H}_5\text{OH}$; therefore, it is easy to judge that the spectrum is strongly related to $\text{C}_2\text{H}_5\text{OH}$. The peak searching and correlation coefficients calculated results show that all the four experimental gases can be correctly recognized in three groups of experiment, and the identification rate of the mixed²² gases spectra is 100%.

The number of sources, also known as the number of independent components (ICs), needs to be evaluated before ICA decomposition. The number of observed signals, as the input of ICA, should be equal to or greater than the actual number of components in the mixture; otherwise, the ICA results will have error. There are many researches²³ about how to evaluate the number of components in chemical mixture. The number of components exist in the actual atmosphere can be evaluated by the singular value decomposition of the de-noised spectral matrix, and the number of components is equal with the number of singular values that are higher than a certain threshold. Because the singular vector contains more useful information than the singular value, it is more accurate to judge the source number through the singular vector. Therefore, the specific source number of the atmosphere spectra can be determined by comparing the singular vector waveform after decomposition²⁴. From the first eight singular vectors obtained from singular value decomposition of the atmospheric spectral matrix; we can see that the first five singular vectors have obvious waveforms, but from the sixth singular vector, they fluctuate slightly near zero. According to the result of singular value decomposition, the number of components in atmospheric spectra can be determined to be 5.

Because the specific gases in the actual atmosphere²⁵ are unknown, the component identification of atmospheric spectra can be achieved through calculating and comparing the correlation coefficient between the separated spectra and all the gas spectra with absorption peaks in the waveband of 2800 cm^{-1} – 3200 cm^{-1} . The gaseous pollutants²⁶ in the measurement site were mainly vehicle exhaust, so we compared the separated spectra with the standard spectra of common VOCs in vehicle exhaust, and recorded the gas type corresponding to the maximum value of correlation coefficient. Table 4 lists identification results of separated spectra.

Identification results of separated spectra.

According to the identification results from the correlation coefficient between the separated spectra and the standard spectra, it can be concluded that the five gases existed in the atmospheric were *o*-xylene (C_8H_{10}), methane (CH_4), toluene (C_7H_8), *p*-xylene (C_8H_{10}), and *n*-hexane (C_6H_{14}), respectively. Compared with the analysis results of build-in software of spectrometer, which are based on the classical least squares algorithm, all of the five gases existed in the atmospheric spectra. At the same time, according to the software analysis result, there were traces of benzene and styrene²² in the atmosphere, which were not identified by the ICA separation. The reason for this may be that the concentration²⁷ of the two gases had not changed in the selected spectral samples, so the absorption peaks of the two gases were eliminated by the division operation during the background spectra elimination process.

From the separation results, we can see that ICA algorithms can separate single gas spectrum from heavily overlapped spectra; it can transform²⁸ the spectra set into independent absorption peaks. The results also show that the sequence and amplitude of the results obtained by the ICA algorithm are uncertain. Although the ICA algorithm has good performance on extracting the source signal, the separated signals have uncertain scaling factors. Besides, the absorbance of gas is not in direct proportion to its concentrations in practice. Therefore,

establishing a quantitative spectral model by multiple linear regression²⁹ is necessary for obtaining the concentration information of each pollutant. The common quantitative spectral methods include partial least squares (PLS), classical least squares (CLS), stepwise regression analysis (SRA), and support vector machine (SVR). It is noteworthy that only several spectral samples are needed to complete the whole identification process by the separation algorithm. Conversely, the neural network algorithm and other identification methods like CLS require multiple samples for modeling. Thus, the proposed method is more suitable in practice when reference substances are not available or are expensive. Moreover, the spectral separation process does not depend on the existing spectral database. When the separated spectra are not included in the spectral database, they may belong to new species. We can thus enrich the spectral database by adding the spectra of new species into the existing database.

The identification results of actual atmospheric spectra show that the ICA method can effectively identify the gaseous pollutants whose concentration changes in the measured spectra. Because the absorption peaks of gas spectrum with constant concentration would be eliminated by the background spectrum elimination method used in this study, we need to focus on the background spectrum elimination method, which can eliminate the background spectrum³⁰ while retaining all target gas information in the following study, and the selection of proper waveband for ICA separation can reduce the difficulty of spectra identification.

Conclusion

Because the absorption peaks of different gas infrared spectra overlap extensively, the traditional atmospheric spectral detection methods have difficulties rapidly and accurately distinguishing specific gas types from overlapping spectra when monitoring atmospheric gaseous pollutants. In this study, we use the source information recovery ability of ICA algorithm to separate single gas spectra from seriously overlapped, multicomponent FTIR spectra. A series of pretreatments are presented to combat the noise and interference produced in the spectral acquisition process, and experiments on laboratory obtained spectra and actual atmospheric spectra verify the effectiveness of ICA algorithm on mixed spectra separation. The proposed method can improve the identification rate as well as the identification speed and enrich the spectral library compared with traditional gaseous spectral identification methods. The whole separation process only needs several mixed spectral samples, and it can make the online atmospheric spectral monitoring and other linear system analysis with high real-time requirements simpler and more effective. Aerosol particles are airborne solid or liquid particles in the size range of a few nanometers to tens of micrometers. They can be emitted directly into the atmosphere (primary particles), and can also be formed in the atmosphere (secondary particles) by chemical transformation of gaseous precursors such as SO₂, NO_x, and volatile organic compounds. Aerosol particles are of great concerns due to their environmental, health, climatic and biogeochemical impacts. Water, which can exist in gas, liquid and solid states, is ubiquitous in the troposphere. Interactions of water vapor with aerosol particles largely affect the roles that aerosol particles play in the Earth system. When water vapor is supersaturated (i.e. when relative humidity, RH, is >100%), aerosol particles can act as cloud condensation nuclei (CCN) to form cloud droplets and as ice-nucleating particles (INPs) to form ice crystals. Cloud condensation nucleation and ice nucleation activities of aerosol particles, as well as relevant experimental techniques, have been recently reviewed in ability of a substance to absorb/adsorb water as a function of RH is typically termed as

A single-component particle which contains one of water soluble inorganic salts, such as (NH₄)₂SO₄ and NaCl, is solid at low RH. When RH is increased to the deliquescence relative humidity (DRH), the solid particle will undergo deliquescence to form an aqueous particle, and the aqueous particle at DRH is composed of a saturated solution. Further increase in RH would increase the water content of the aqueous droplet, i.e. the aqueous particle would become more diluted as RH increases. During humidification thermodynamics determines phase transition and hygroscopic growth of the particle. During dehumidification, an aqueous particle would not undergo efflorescence to form a solid particle when RH is decreased to below DRH; instead, the aqueous particle would become supersaturated. Only when RH is further decreased to efflorescence relative humidity (ERH), the aqueous particle would undergo crystallization, leading to the formation of a solid particle. Therefore, efflorescence is also kinetically controlled and there is a hysteresis between

deliquescence and efflorescence. Deliquescence and efflorescence of multicomponent particles can be more complicated. It should be pointed out that not all the single-component particles exhibit distinctive deliquescence and efflorescence. Instead, continuous uptake or loss of liquid water is observed during humidification and dehumidification processes for many inorganic and organic particles. Particles with extremely low hygroscopicity (e.g., mineral dust) will not be deliquesced even at very high RH; instead, adsorbed water will be formed on the particle surface.

References

- 1 Cairong Lou PMID: 29063278 DOI: 10.1007/s10661-017-6281-z humidity
- 2 Hernandez, G., Berry, T-A., Wallis, S.L., & Poyner, D. (2017, November) <https://hdl.handle.net/10652/4299>
3. Environmental Engineering, Vol. 102 (2017) DOI: 10.7763/IPCBE. 2017. V102. 8
4. Cohen, H. Anderson, B. Ostra, K. Pandey, M. Krzyznowski, N. Künzli, K. Gutschmidt, A. Pope, I. Romieu, J. Samet, K. Smith. Environ. Health. 2005, 68: 1-7
5. K. Donaldson, V. Stone, A. Seaton, W. Mac Nee. Health. 2001, 109: 523-527
6. Abdi, H., and Williams, L. J. (2010). Principal Component Analysis. Wiley Interdisciplinary Rev.: Comput. Statist., 2:433–459. [Crossref], [Google Scholar]
7. Allen, D. T., Palen, E. J., Haimov, M. I., Hering, S. V., and Young, J. R. (1994). Fourier Transform Infrared Spectroscopy of Aerosol Collected in a Low Pressure Impactor Method Development and Field Calibration. Aerosol Sci. Technol., 21:325–342 Baumann,
8. K., Jayanty, R. K. M., and Flanagan, J. B. (2008). Fine Particulate Matter Source Apportionment for the Chemical Speciation Trends Network Site at Birmingham, Alabama, . J. Air Waste Manag. Assoc., 58:27–44. [Taylor & Francis Online],
9. Blando, J. D., Porcja, R. J., and Turpin, B. J. (2001). Issues in the Quantitation of Functional Groups by FTIR Spectroscopic Analysis of Impactor-Collected Aerosol Samples. Aerosol Sci. Technol., 35:899–908. [Taylor & Francis Online], [Web of Science ®],
10. Bocklitz, T., Walter, A., Hartmann, K., Rosch, P., and Popp, J. (2011). How to Pre-Process Raman Spectra for Reliable and Stable Models? Anal. Chim. Acta, 704:47–56. [Crossref], [PubMed], [Web of Science ®],
11. Boer, G. J., Sokolik, I. N., and Martin, S. T. (2007). Infrared Optical Constants of Aqueous Sulfate–Nitrate–Ammonium Multi-Component Tropospheric Aerosols from Attenuated Total Reflectance Measurements—Part I: Results and Analysis of Spectral Absorbing Features. J. Quant. Spectrosc. Radiat. Transfer, 108:17–38.
12. Cai, W., Li, Y., and Shao, X. (2008). A Variable Selection Method Based on Uninformative Variable Elimination for Multivariate Calibration of Near-Infrared Spectra. Chemom. Intell. Lab. Syst. 90:188–194.
13. Carlton, A. G., Turpin, B. J., Altieri, K. E., Seitzinger, S. P., Mathur, R., Roselle, S. J., and Weber, R. J. (2008). CMAQ Model Performance Enhanced When in-Cloud Secondary Organic Aerosol is Included: Comparisons of Organic Carbon Predictions with Measurements. Environ. Sci. Technol., 42:8798–8802.
14. Centner, V., Massart, D.-L., de Noord, O. E., de Jong, S., C. (1996). Elimination of

- Uninformative Variables for Multivariate Calibration. *Anal. Chem.*, 68:3851–3858.
15. Chen, Z.-P., Li, L.-M., Yu, R.-Q., Littlejohn, D., Nordon, A., Morris, J., Dann, A. S., Jeffkins, P. A., Richardson, M. D., and Stimpson, S. L. (2011). Systematic Prediction Error Correction: A Novel Strategy for Maintaining the Predictive Abilities of Multivariate Calibration Models. *Analyst*, 136:98–106.
 16. Satorre, M. A., Palumbo, M. E., & Strazzulla, G. 2000, *Ap&SS*, 274, 643
 17. Slinger, T. G., Wood, B. J., & Black, G. 1972, *J. Chem. Phys.*, 57,
 18. Species: the effect of temperature, *Atmos. Chem. Phys.*, 19, 2247-2258, 2019.
 19. Thomas, E., Rudich, Y., Trakhtenberg, S., and Ussyshkin, R.: Water adsorption by
 20. Hydrophobic organic surfaces: Experimental evidence and implications to the atmospheric
 21. Properties of organic aerosols, *J. Geophys. Res.-Atmos.*, 104, 16053-16059,
 22. Thomas, S., Cole, M., Villa-Lopez, F. H., and Gardner, J. W.: High frequency surface
 23. Spectroscopy, *J. Phys. Chem. A*, 114, 12237-12243, 2010
 25. Aerosol hygroscopic properties, *Atmos. Meas. Tech.*, 10, 1269-1280, 2017.
 26. *Aerosol Science and Technology* Volume 50, 2016 - Issue 10 AT Weakley · 2016 ·
 27. J. R. Hodgkinson and P. Tatam, “Optical gas sensing: a review,” *Measurement Science and Technology*, vol. 24, no. 1, Article ID 012004, 2013.
 28. S. K. Akagi, I. R. Burling, A. Mendoza et al., “Field measurements of trace gases emitted by prescribed fires in southeastern US pine forests using an open-path FTIR system,” *Atmospheric Chemistry and Physics*, vol. 14, no. 1, pp. 199–215, 2014.
 29. Recent advances in aerosol analysis by infrared spectroscopy Author links open overlay panel David T.Allen EdwardPale
 30. Centner, V., Massart, D.-L., de Noord, O. E., de Jong, S., Vandeginste, B. M., and Sterna, C. (1996).